SPECTROSCOPIC FACTORS IN ^{16}O AND NUCLEON ASYMMETRY

C. BARBIERI

Theoretical Nuclear Physics Laboratory, RIKEN Nishina Center, 2-1 Hirosawa, Wako, Saitama 351-0198 Japan

W. H. DICKHOFF

Department of Physics, Washington University, St. Louis, Missouri 63130, USA

Received 15 January 2009

The self-consistent Green's functions method is employed to study the spectroscopic factors of quasiparticle states around ^{16,28}O and ^{40,60}Ca. The Faddeev random phase approximation (FRPA) is used to account for the coupling of particles with collective excitation modes. Results for ^{16}O are reviewed first. The same approach is applied to isotopes with large proton-neutron asymmetry to estimate its effect on spectroscopic factors. The results, based on the chiral N3LO force, exhibit an asymmetry dependence similar to that observed in heavy-ion knockout experiments but weaker in magnitude.

Keywords: Nuclear correlations; spectroscopic factors; proton-neutron asymmetry.

1. Introduction

In the independent particle model (IPM) of atomic nuclei, protons and neutrons move freely in a common mean-field potential. Obviously, this is an approximate picture since the residual interaction smears the Fermi surface and leads to partial occupation of each orbit. For states close to the Fermi level, this effect is observed through a reduction of the experimental knockout and pickup cross sections. Experimental spectroscopic factors (SFs) are defined as the quenching of the observed reaction rate with respect to that calculated assuming full occupancy. Hence, they are interpreted as the occupation of a given orbit. However, from a strict theoretical point of view SFs are not occupation numbers. Instead, they give a "measure" of what fraction of the *final* wave function can be factorized into a (correlated) core plus an independent particle or hole state. Strong deviations from unity signal the onset of substantial correlation effects and imply the existence of non trivial many-body dynamics.

As far as stable nuclei are concerned, a large body of data has been accumulated from $(e,e'p)$ experiments yielding the best estimates of absolute spectroscopic factors. These studies showed that proton SFs for isotopes all across the nuclear

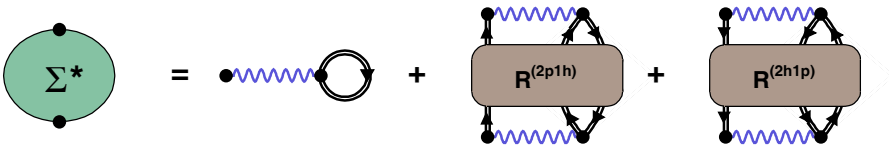

Fig. 1. Diagrams contributing to the irreducible self-energy $\Sigma^\star(\omega)$. The double lines represent a dressed propagator and the wavy lines correspond to a G-matrix (that is used in this work as an effective interaction). The first term is the Brueckner-Hartree-Fock potential while the others represent two-particle–one-hole / two-hole–one-particle (2p1h/2h1p) or higher contributions that are approximated through the Faddeev RPA equations.

chart are uniformly quenched to 60-70% of the IPM value [1,2]. This information is however limited to protons and stable isotopes. More recently, experimental information on SFs of dripline isotopes has been obtained by means of nucleon knockout using intermediate energy heavy-ion beams [3,4]. These results also include neutron data, and suggest a strong dependence of SFs on the N/Z ratio.

In nuclear structure studies, one usually distinguishes between short-range (SRC) and long-range and correlations (LRC). The former are induced by the strong repulsive core and the tensor component of the nuclear force at small distances. These remove strength from the Fermi sea to very high energies and momenta and have long been proposed as one possible mechanism for the quenching of SFs. However, different theoretical evaluations predicted that SRC can account for at most a 10-15% reduction (see Refs. [5,6] for ^{16}O). This result is now supported by electron scattering experiments [7] at high energies, where the reactions can be analyzed using a Glauber-inspired approach [8,9,10] (see also Ref. [11]). Calculations like those reported in Sec. 3 shows that the largest part of the quenching is instead due to LRC. In particular, couplings between single nucleons and collective surface phonons is important [12].

This talk reviews our theoretical understanding of SFs obtained from calculations based on Green's function theory. The formalism used in these studies is summarized in Sec. 2 and its application to ^{16}O, as a test case, is discussed in Sec. 3. Sec. 4 reports on a first investigation of correlations in asymmetric isotopes.

2. Faddeev-RPA Method

We consider the calculation of the single-particle (sp) Green's function [13]

$$g_{\alpha\beta}(\omega) \;=\; \sum_n \frac{(\mathcal{X}^n_\alpha)^*\;\mathcal{X}^n_\beta}{\omega-(E^{A+1}_n-E^A_0)+i\eta} \;+\; \sum_k \frac{\mathcal{Y}^k_\alpha\;\left(\mathcal{Y}^k_\beta\right)^*}{\omega-(E^A_0-E^{A-1}_k)-i\eta}\,, \qquad (1)$$

where $\mathcal{X}^n_\alpha = \langle\Psi^{A+1}_n|c^\dagger_\alpha|\Psi^A_0\rangle$ ($\mathcal{Y}^k_\alpha = \langle\Psi^{A-1}_k|c_\alpha|\Psi^A_0\rangle$) are the spectroscopic amplitudes for the excited states of a system with $A+1$ ($A-1$) particles. In these definitions, $|\Psi^{A+1}_n\rangle$, $|\Psi^{A-1}_k\rangle$ are the eigenstates, and E^{A+1}_n, E^{A-1}_k the eigenenergies of the $(A\pm1)$-nucleon system. Therefore, the poles of the sp propagator

reflect the energy transfer observed in pickup and knockout reactions. The corresponding SFs for transitions to a quasihole (quasiparticle) state are obtained as $Z_k = \sum_\alpha \left|\mathcal{Y}^k_\alpha\right|^2$ ($Z_n = \sum_\alpha |\mathcal{X}^n_\alpha|^2$).

The one-body Green's function is computed by solving the Dyson equation

$$g_{\alpha\beta}(\omega) = g^0_{\alpha\beta}(\omega) \; + \; \sum_{\gamma\delta} g^0_{\alpha\gamma}(\omega)\Sigma^\star_{\gamma\delta}(\omega) g_{\delta\beta}(\omega) \;\; , \tag{2}$$

where the irreducible self-energy $\Sigma^\star_{\gamma\delta}(\omega)$ acts as an effective, energy-dependent, potential. The latter can be expanded in a Feynman-Dyson series [13] in terms of the exact propagator $g_{\alpha\beta}(\omega)$, which itself is a solution of Eq. (2). In this expansion, $\Sigma^\star_{\gamma\delta}(\omega)$ can be represented as shown in Fig. 1 by the sum of a Hartree-Fock-like potential and the polarization propagator, $R(\omega)$, that account for deviations from the mean-field [12]. It is at the 2p1h/2h1p level that the correlations involving couplings of sp to collective modes need to be included. The SCGF approach is initiated by solving the self-energy and the Dyson Eq. (2) in terms of an unperturbed propagator (e.g. Hartree-Fock). The (dressed) solution $g_{\alpha\beta}(\omega)$ is then taken as a new input and the whole calculation is iterated until convergence is reached.

2.1. *Faddeev RPA method for the self-energy*

The polarization propagator $R(\omega)$ can be expanded in terms of simpler Green's functions that involve the propagation of one quasiparticle [Eq. (1)] or more. This approach has the advantage that it allows the identification and inclusion of key physics ingredients of the many-body dynamics. By truncating to particular subsets of diagrams, one can then construct suitable approximations to the self-energy. Moreover, since infinite sets of linked diagrams are summed, the approach is non-perturbative and satisfies the extensivity condition. This expansion also serves as a guideline for systematic improvements of the method.

In the following we are interested in describing the coupling of sp motion to particle-hole (ph) and particle-particle (hole-hole) [pp(hh)] collective excitations of the system. Following Refs. [14,15], we first consider the ph polarization propagator describing excited states in the A-particle system

$$\begin{aligned}\Pi_{\alpha\beta,\gamma\delta}(\omega) = &\sum_{n\neq 0} \frac{\langle\Psi^A_0|c^\dagger_\beta c_\alpha|\Psi^A_n\rangle \, \langle\Psi^A_n|c^\dagger_\gamma c_\delta|\Psi^A_0\rangle}{\omega - \left(E^A_n - E^A_0\right) + i\eta} \\ &- \sum_{n\neq 0} \frac{\langle\Psi^A_0|c^\dagger_\gamma c_\delta|\Psi^A_n\rangle \, \langle\Psi^A_n|c^\dagger_\beta c_\alpha|\Psi^A_0\rangle}{\omega - \left(E^A_0 - E^A_n\right) - i\eta} \;\; ,\end{aligned} \tag{3}$$

and the two-particle propagator, for the addition/removal of two particles

$$\begin{aligned}g^{II}_{\alpha\beta,\gamma\delta}(\omega) = &\sum_{n} \frac{\langle\Psi^A_0|c_\beta c_\alpha|\Psi^{A+2}_n\rangle \, \langle\Psi^{A+2}_n|c^\dagger_\gamma c^\dagger_\delta|\Psi^A_0\rangle}{\omega - \left(E^{A+2}_n - E^A_0\right) + i\eta} \\ &- \sum_{k} \frac{\langle\Psi^A_0|c^\dagger_\gamma c^\dagger_\delta|\Psi^{A-2}_k\rangle \, \langle\Psi^{A-2}_k|c_\beta c_\alpha|\Psi^A_0\rangle}{\omega - \left(E^A_0 - E^{A-2}_k\right) - i\eta} \;\; .\end{aligned} \tag{4}$$

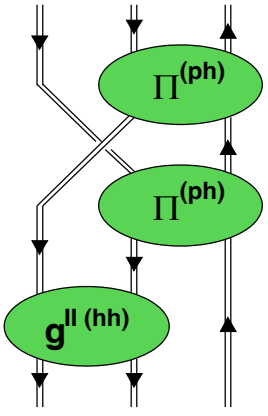

Fig. 2. Example of a diagram appearing in the all-order summation generated by the set of Faddeev equations. This diagram contributes to the $R^{2h1p}(\omega)$ propagator seen in Fig. 1.

In the calculation of Sec. 3, these have been approximated by solving the dressed random phase approximation (DRPA) equations [13], which account for the effects of the strength distribution of the particle and hole fragments.

The ph (3) and pp(hh) (4) propagators are inserted in the self-energy by solving a set of Faddeev equations for the 2p1h and 2h1p propagators of Fig. 1. The details of the Faddeev RPA (FRPA) approach are given in Ref. [14,15]. For the present discussion it is sufficient to note that collective excitations are coupled to sp propagators generating an infinite series of diagrams, including the one shown in Fig. 2.

3. Hole Spectroscopic Factors for ^{16}O

The calculations for ^{16}O, in Ref. [16], were performed in an harmonic oscillator basis with parameter $b = 1.76$ fm (corresponding to $\hbar\omega = 13.4$ MeV). The first four major shells (from $0s$ to $1p0f$) plus the $0g_{9/2}$ orbit where included. Inside the model space, a Brueckner G-matrix derived from the Bonn-C potentialwas used as an effective interaction. The short-range core of this NN interaction induces an additional 10% reduction of the spectroscopic factors for main quasiparticle peaks, by moving strength to very high energies [12]. This effect was included in the solution of the Dyson equation by treating the energy dependence of the G-matrix explicitly.

The FRPA calculations were then iterated to self-consistency, thus including the effects of fragmentation. In doing this, the largest fragments that appear—close to the Fermi energy—in the (dressed) sp propagator, Eq. (1), are maintained. The remaining strength is collected, at each iteration, into effective poles [16].

3.1. *Spectroscopic factors and role of low excited states in* ^{16}O

The one-hole strength distribution obtained upon convergence of the SCGF is shown in Fig. 3, where it is compared with the experiment (top panels). Similar results are obtained for the particle strength, including large peaks near the Fermi surface and

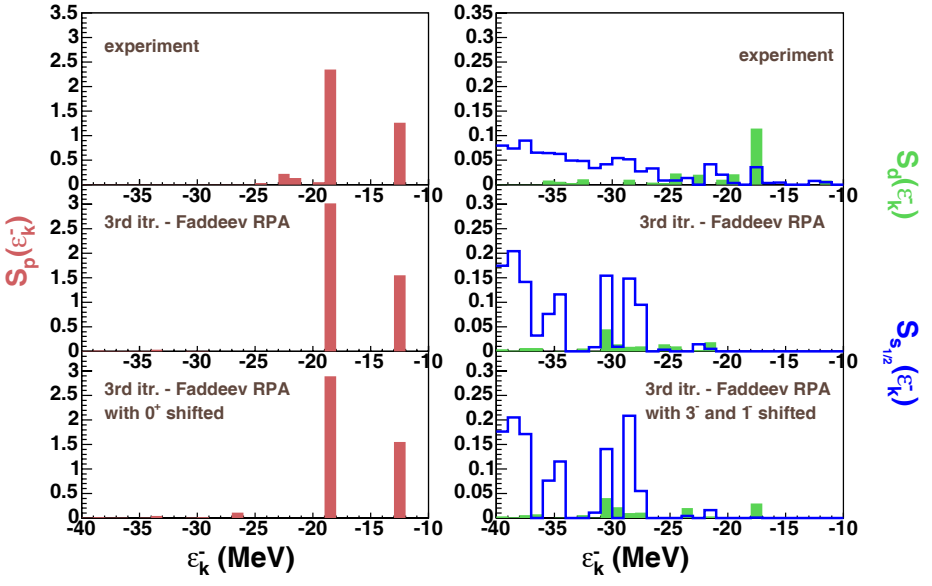

Fig. 3. One-proton removal strength as a function of the hole sp energy $\varepsilon_k^- = E_0^A - E_k^{A-1}$ for ^{16}O for angular momenta $\ell = 1$ (left) and $\ell = 0, 2$ (right). For the positive parity states, the solid bars correspond to results for $d_{5/2}$ and $d_{3/2}$ orbitals, while the thick lines refer to $s_{1/2}$. The top panels show the experimental values taken from [17]. The central panels give the theoretical results for the self-consistent spectral function. The bottom panels show the results obtained by constraining the lowest excited states [i.e. the poles of Eq. (3)], to the corresponding experimental energies. A small amount of $p_{3/2}$ strength is observed experimentally at around -23 MeV (top panel) and obtained theoretically at -26 MeV (bottom panel).

a fragmented distribution at larger energies. The spectroscopic factors obtained for removal of a proton amount to 0.75 of the IPM value for the $p_{3/2}$ peak and 0.77 for the $p_{1/2}$. These refer to the middle panels of this figure.

Failures to fully reproduce the observed removal strength can be traced to the difficulties of the RPA to describe the low-energy spectrum. To clarify this point we repeated the above calculations of the sp propagator by shifting, at each iteration, the first RPA 0^+ eigenstate in ^{16}O. This eigenvalue is obtained at larger energies but the corresponding pole of Eq. (3) was constrained to the experimental energy of the first excited state. This is expected to represent qualitatively the cluster state which is also excited by a M(E0) transition (see e.g. the contribution of Funaki and Schuck to these proceedings).[a] This change leads to the appearance of satellite $p_{3/2}$ fragments around -26.3 MeV, which might be identified with the fragments seen

[a]The RPA wave function is a particle-hole configuration and is intrinsically different from the experimental first excited level, which is a cluster state. However, both states are strongly excited by one-body operators. Since this is the mechanism that couples nucleons to collective modes in the FRPA, Fig. 2, the two are expected to have similar effects on the results discussed here.

Table 1. Dependence of theoretical spectroscopic factors (as a fraction of the IPM value) on the inclusion of various SRC and LRC effects. The value in parentheses is the summed strength of small $p_{3/2}$ fragments near the quasihole peak.

Spectroscopic factors of ^{16}O	$Z_{p1/2}$	$Z_{p3/2}$
SRC only [5,6]	∼0.90	∼0.90
SRC + LRC(FRPA + sp dressing) [16]	0.77	0.75
SRC + LRC(FRPA + sp dressing + 0_2^+ state) [16]	0.77	0.72(0.026)
Experiment [18,19]	0.64-0.71	0.54-0.61

experimentally at slightly higher energy. These are calculated to have total strength of 2.6%, while the dominant peak is reduced to 0.72 (see Table 1). The associated spectral function is shown in the lower-left panel of Fig. 3. Thus one concludes that the additional $p_{3/2}$ fragments are generated by propagating a hole on top of excited 0^+ level of the ^{16}O core.

The other two low-lying states of ^{16}O that may be of some relevance are the isoscalar 1^- and 3^-, and are calculated at ∼3 MeV above the experimental value. Constraining their energies to the experimental values leads to analogous improvements. In particular a $d_{5/2}$ hole peak is obtained at a missing energy of -17.7 MeV, in nice agreement with the experiment (lower-right panel in Fig. 3).

3.2. *Status of theoretical calculations for ^{16}O*

The contributions to the reduction of SFs are summarized in Table 1 for the p shell orbits of ^{16}O. The range of values labeled as "experiment" reflects the quenching factors *needed* by theoretical analyses to reproduce the observed $(e,e'p)$ data. As mentioned in Sec. 1, SRC account for a modest part of the reduction of SFs. For the case of hole states in ^{16}O, both Green's function theory [5] and variational Monte Carlo [6] methods predict a 10% depletion. The agreement between different methods and interactions (Bonn and Argonne forces were used) give us confidence that short-range physics is under control and that, at low energies, its overall effect exhibits little dependence on how realistic forces are modeled. The calculations of Sec. 3.1 shows that the largest part of the quenching is instead due to LRC effects, such as couplings between single nucleons and collective surface phonons and configuration mixing in the valence shell. Based on the findings of Ref. [16], it is plausible that clustering degrees of freedom are the missing ingredient in this particular isotope. We note that ^{16}O is an exceptionally difficult nucleus in this respect and so far it has defeated a complete theoretical understanding of knockout cross sections. Thus it provides a stringent benchmark for theoretical calculations. Successful calculations have been obtained for other nuclei [20,21].

4. Extension to Larger Systems and Asymmetric Nuclei

Experimental and theoretical studies of electron scattering reactions have led to a global picture of the properties of protons for stable nuclei [12]. The first information

on how these features change toward the driplines has only recently become available. In particular, one-nucleon knockout experiments in inverse kinematics have found that SFs do change with proton-neutron asymmetry. In general, the quenching of quasiparticle orbits (and hence correlations) become stronger with increasing separation energy [4].

The extension of FRPA calculations from ^{16}O to large isotopes faces technical challenges due to the increasing model space and computational load. A first breakthrough has been obtained in Ref. [22], where self-consistent calculations of ^{16}O were obtained in a large basis (up to 8 oscillator shells). Similar calculations can now be performed in the pf shell. In this case self-consistency is implemented only partially (for now), according to Ref. [23].

Figure 4 shows first FRPA results for the spectroscopic factors of quasiparticles around ^{16,28}O and ^{40,60}Ca. These are obtained form a G-matrix [24] based on the chiral N3LO interaction and following the calculation scheme of Ref. [23]. A dependence on the proton-neutron asymmetry is indeed observed in the FRPA, with the spectroscopic factors becoming smaller with increasing nucleon separation energy. A dispersive optical model analysis, which is constrained to data up to ^{48}Ca, has also been extrapolated to proton rich Ca isotopes, with similar findings [25,26]. However, for both analyses the change in magnitude is significantly smaller than the one deduced from direct knockout data [4]. The most asymmetric isotope in Fig. 4 is ^{28}O with an asymmetry parameter $\alpha = (N - Z)/A \approx 0.43$. In this case, the FRPA SFs for knockout of a proton and a neutron differ by about 11% of the IPM. This result is in agreement with calculations of nuclear matter where, however, the only mechanism considered was SRC [27]. It must be stressed that collective excitations

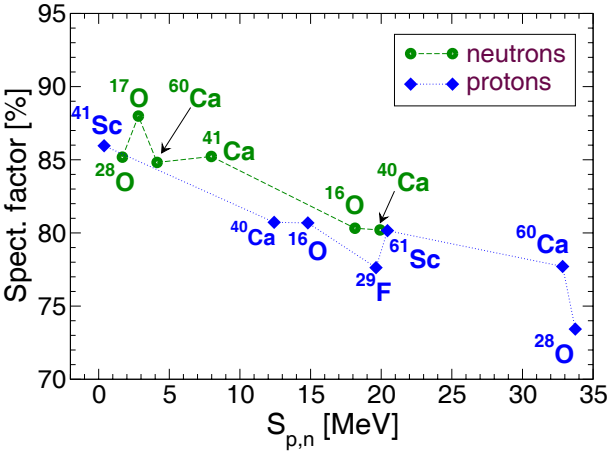

Fig. 4. SFs obtained from partially self-consistent FRPA. All numbers are given as a fraction of the IPM value and refer to transitions from ground state to ground state. The points refer to knockout of a nucleon from the isotope indicated nearby. The lines are a guide to the eye.

are the most important degrees of freedom governing the reduction of SFs. These are properly accounted for by the FRPA approach. However, realistic two-nucleon forces such as the one used here have a tendency to overestimate the excitation energy of giant resonances, and therefore to underestimate their importance. It is plausible that the dependence on asymmetry seen in Fig. 4 will become more substantial once FRPA calculations with improved forces will be available.

5. Conclusions

The Faddeev RPA method has been used to investigate the effects of SRC and couplings of nucleons to collective excitations. The latter give the most substantial contribution to the quenching of spectroscopic factors. Applications to asymmetric isotopes shows a reduction of the SFs for quasiparticle orbits with increasing separation energy. This dependence is considerably weaker than the one deduced from heavy-ion knockout experiments. It is argued that improved forces and calculations will be needed to resolve this issue.

Acknowledgments

This work was in part supported by the U.S. National Science Fundation under Grant no. PHY-0652900.

References

1. L. Lapikás, Nucl. Phys. **A553**, 297c (1993).
2. G. J. Kramers, H. P. Blok, and L. Lapikás, Nucl. Phys. **A679**, 267 (2001).
3. P. G. Hansen and J. A. Tostevin, Ann. Rev. Nucl. Part. Sci. **53**, 219 (2003).
4. A. Gade, *et al.*, Phys. Rev. C **77**, 0044306 (2008).
5. H. Müther, A. Polls, and W. H. Dickhoff, Phys. Rev. C **51**, 3040 (1995).
6. D. Van Neck,*et al.*, Phys. Rev. C **57**, 2308 (1998).
7. D. Rohe, *et al.*, Phys. Rev. Lett. **93**, 182501 (2004).
8. C. Barbieri and L. Lapikás, Phys. Rev. C **70**, 054612 (2004).
9. C. Barbieri, D. Rohe, I. Sick, and L. Lapikás, Phys. Lett. **B608**, 47 (2005).
10. C. Barbieri, Nucl. Phys. B (Proc. Suppl.) **159**, 174 (2006).
11. R. Subedi *et al.*, Science **320**, 1476 (2008).
12. W. H. Dickhoff and C. Barbieri, Prog. Part. Nucl. Phys. **52**, 377 (2004).
13. W. H. Dickhoff and D. Van Neck, *Many-Body Theory Exposed!*, 2nd ed. (World Scientific, Singapore, 2008).
14. C. Barbieri and W. H. Dickhoff, Phys. Rev. C **63**, 034313 (2001).
15. C. Barbieri, D. Van Neck and W. H. Dickhoff, Phys. Rev. A **76**, 052503 (2007).
16. C. Barbieri and W. H. Dickhoff, Phys. Rev. C **65**, 064313 (2002).
17. M. Leuschner *et al.*, Phys. Rev. C **49**, 955 (1994).
18. M. Radici, W. H. Dickhoff, and E. Roth Stoddard, Phys. Rev. C **66**, 014613 (2002).
19. M. Radici, A. Meucci and W. H. Dickhoff, Eur. Phys. J. **A 17**, 65 (2003).
20. G. A.Rijsdijk, K Allaart, and W. H. Dickhoff, Nucl. Phys. **A550**, 159 (1992).
21. L. Lapikás, J. Wesseling, and R. B. Wiringa, Phys. Rev. Lett. **82**, 4404 (1999).
22. C. Barbieri, Phys. Lett. **B643**, 268 (2006).

23. C. Barbieri and M. Hjorth-Jensen, in preparation.
24. M. Hjorth-Jensen, T. T. S. Kuo, and E. Osnes, Phys. Rep. **261**, 125 (1995).
25. R. J. Charity *et al.*, Phys. Rev. Lett. **97**, 162503 (2006).
26. R. J. Charity *et al.*, Phys. Rev. C **76**, 044314 (2007).
27. T. Frick *et al.*, Phys. Rev. C **71**, 014313 (2005).